The EMBO Journal Vol.17 No.12 pp.3297–3308, 1998

A neuronal two P domain K^+ channel stimulated by arachidonic acid and polyunsaturated fatty acids

Michel Fink, Florian Lesage, Fabrice Duprat, Catherine Heurteaux, Roberto Reyes, Michel Fosset and Michel Lazdunski[1]

Institut de Pharmacologie Moléculaire et Cellulaire–CNRS–UPR 411, 660 route des Lucioles, Sophia Antipolis, 06560 Valbonne, France

[1]Corresponding author
e-mail: ipmc@ipnmc.cnrs.fr

M.Fink, F.Lesage and F.Duprat contributed equally to this work

TWIK-1, TREK-1 and TASK K^+ channels comprise a class of pore-forming subunits with four membrane-spanning segments and two P domains. Here we report the cloning of TRAAK, a 398 amino acid protein which is a new member of this mammalian class of K^+ channels. Unlike TWIK-1, TREK-1 and TASK which are widely distributed in many different mouse tissues, TRAAK is present exclusively in brain, spinal cord and retina. Expression of TRAAK in *Xenopus* oocytes and COS cells induces instantaneous and non-inactivating currents that are not gated by voltage. These currents are only partially inhibited by Ba^{2+} at high concentrations and are insensitive to the other classical K^+ channel blockers tetraethylammonium, 4-aminopyridine and Cs^+. A particularly salient feature of TRAAK is that they can be stimulated by arachidonic acid (AA) and other unsaturated fatty acids but not by saturated fatty acids. These channels probably correspond to the functional class of fatty acid-stimulated K^+ currents that recently were identified in native neuronal cells but have not yet been cloned. These TRAAK channels might be essential in normal physiological processes in which AA is known to play an important role, such as synaptic transmission, and also in pathophysiological processes such as brain ischemia. TRAAK channels are stimulated by the neuroprotective drug riluzole.

Keywords: arachidonic acid/background conductance/electrophysiology/*in situ* hybridization

Introduction

Potassium channels play a key role in numerous cellular functions in excitable and non-excitable cells (Rudy, 1988; Hille, 1992; Quast and Weston, 1994; Barnard, 1996). Among all ion channels, they form the largest family in terms of both structure and function. Cloning has led to the isolation and functional expression of a wide variety of subunits that form K^+ channels. These subunits are now classically separated into three different structural classes. The first to be identified were the *Shaker* family (Pongs, 1992; Jan and Jan, 1994) and the Kir family (Fakler and Ruppersberg, 1996; Isomoto *et al.*, 1997; Nichols and Lopatin, 1997). *Shaker*-type channels contain a conserved hydrophobic core with six transmembrane segments (TMS) whereas Kir channels have only two TMS. The unique common feature of all K^+ channels cloned to date is the presence of a conserved motif called the P domain which is a part of the K^+ conduction pathway (Hartmann *et al.*, 1991; Yool and Schwarz, 1991; Heginbotham *et al.*, 1994; MacKinnon, 1995). Functional *Shaker* and Kir K^+ channels are multimers of four pore-forming subunits (Isacoff *et al.*, 1990; Ruppersberg *et al.*, 1990; Glowatzki *et al.*, 1995; Yang *et al.*, 1995) that can be associated with auxiliary subunits (Kvβ, IsK, SUR) (Inagaki *et al.*, 1995; Pongs, 1995; Barhanin *et al.*, 1996). The third class of K^+ channels, which were first cloned from mammals, is the TWIK family (Fink *et al.*, 1996; Lesage *et al.*, 1996a, 1997; Duprat *et al.*, 1997; Leonoudakis *et al.*, 1998). These new K^+ channels share the same overall structure, consisting of four TMS and two P domains. The presence of two P domains in one subunit suggests that the association of two of these subunits is enough to create a K^+-selective pore (Lesage *et al.*, 1996b). Despite a low sequence similarity and different functional properties, TWIK-related K^+ channels all produce instantaneous and non-inactivating currents that do not display a voltage-dependent activation threshold. They are open at the resting potential and are able to drive the membrane potential near the K^+ equilibrium potential. These properties as well as their wide tissue distribution suggest that these two P domain K^+ channels are background channels that are involved in the generation and modulation of the resting membrane potential in various cell types (Lesage and Lazdunski, 1998).

Here, we report the cloning, tissue distribution and functional expression of TRAAK, a TWIK-related arachidonic acid-stimulated K^+ channel. Expression of TRAAK in adult mouse is restricted to the brain, spinal cord and retina, and its localization in these tissues has been studied by *in situ* hybridization. Like TASK, the TRAAK channels are instantaneous with voltage changes and their current–voltage relationships fit the curves predicted from the constant field theory for simple electrodiffusion through an open K^+-selective pore. The activity of TRAAK currents is strongly increased by arachidonic acid (AA) and by other polyunsaturated fatty acids (FAs). The TRAAK channel is the first AA-stimulated background K^+ channel characterized at the molecular level and shown to be expressed specifically in neuronal cells.

Results

Cloning and primary structure of TRAAK

Searches of DNA databases using the tBlastn alignment program led to the identification of a mouse expressed sequence tag (EST; DDBJ/EMBL/GenBank accession

© Oxford University Press

No. AA155263) of 446 bp. Two specific oligonucleotides were designed to amplify a 330 bp DNA fragment from mouse brain cDNA. This fragment was labeled and used to screen a mouse brain cDNA library. Two independent clones were isolated. The largest cDNA insert (1.6 kb) contains an open reading frame (ORF) of 204 bp that encodes a 67 amino acid polypeptide related to the N-terminus of TREK-1. A second ORF of 885 bp was found to be contiguous to the first one but in another frame. This second ORF encodes the 293 amino acid C-terminus of a two P domain K^+ channel. These results suggested that the cloned 1.6 kb cDNA corresponded to a truncated splice variant. In order to clone the complete protein, primers were chosen upstream and downstream of the putative initiation and stop codons, respectively, and RT–PCR was performed from mouse brain. Two products were amplified, as expected. The shorter PCR product is identical to the cDNA isolated previously, while the longer one contains a 126 bp insertion leading to the formation of a 1197 bp ORF encoding a protein of 398 residues (Figure 1A). The sequence alignment presented in Figure 2 clearly shows that this protein, called TRAAK, belongs to the recently discovered family of TWIK-related K^+ channels. The overall structure contains four potential TMS (M1–M4) and two P domains (P1 and P2). When compared with TWIK-1 and TREK-1, TRAAK has a shorter N-terminus but an extended C-terminus. Like the other two P domain K^+ channels, TRAAK has an extended extracellular loop between M1 and P1, with a cysteine residue at a position (C52) analogous to the cysteine (C69) involved in the disulfide-bridged homodimerization of TWIK-1 (Lesage *et al.*, 1996b). TRAAK contains two consensus sites for N-linked glycosylation (residues 81 and 84) and numerous potential phosphorylation sites for protein kinase A (PKA) (residue 383), protein kinase C (PKC) (residues 146, 262, 284, 288, 360 and 379) and casein kinase II (residues 265, 340 and 358) (Kemp and Pearson, 1990). Most of these potential phosphorylation sites (9 out of 10) are located on the cytoplasmic C-terminus. All these sites are absent in the short splice variant of TRAAK. This variant, called TRAAKt for TRAAK truncated, is identical to TRAAK from residue 1 to 63, and contains four additional residues at the C-terminus resulting from a frameshift (A-M-A-I; Figure 1A). This 67 amino acid truncated form of TRAAK has a single TMS (M1) and a C-terminus corresponding to the extracellular M1–P1 loop, but it lacks a P domain (Figure 1B).

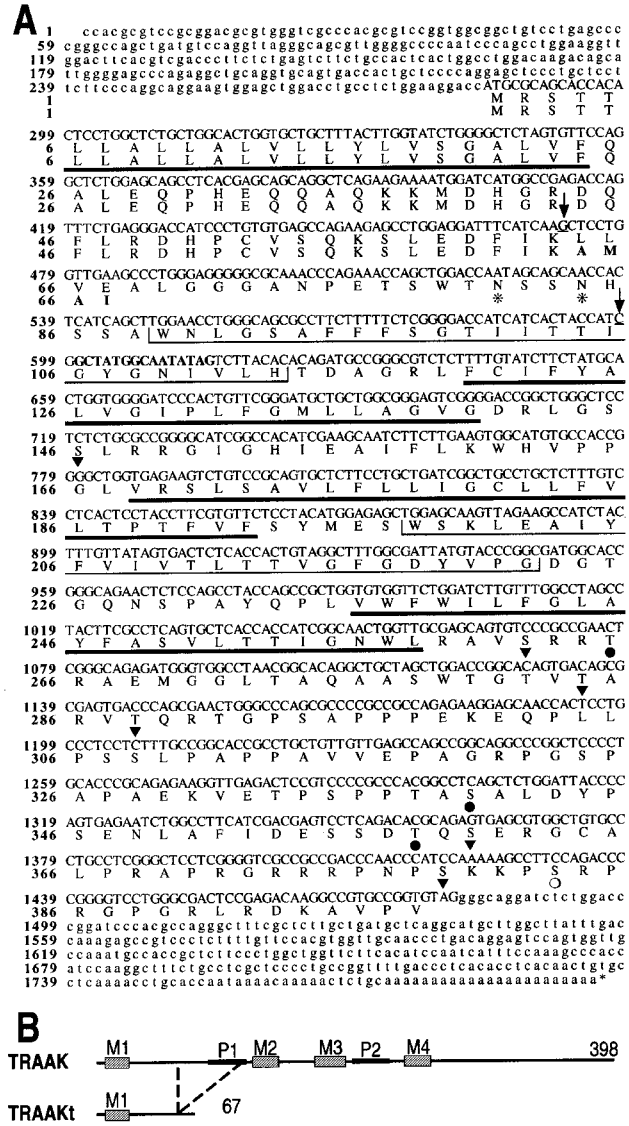

Fig. 1. (**A**) Nucleotide and deduced amino acid sequences of TRAAK and the truncated variant TRAAKt. The four putative TMS (M1–M4) and the two P domains (P1 and P2) are underlined. The arrows and the underlined nucleotides in the nucleic acid sequence indicate the positions where deletion occurred to give TRAAKt. The resulting frameshift in the ORF is shown in bold (nucleotides 600–614) corresponding to four additional residues in the protein TRAAKt (A-M-A-I, in bold) after residue K63. Consensus sites for N-linked glycosylation (*) and phosphorylation by protein kinase C (▼), protein kinase A (○) or casein kinase II (●) are indicated. These sites have been identified using the prosite server (European Bioinformatics Institute) with the ppsearch software (EMBL Data library) based on the MacPattern program. The sequences of TRAAK have been deposited in the DDBJ/EMBL/GenBank database under the accession No. AF056492. (**B**) The deletion that leads to the formation of the truncated form TRAAKt is shown. The truncated form TRAAKt of 67 amino acids contains the M1 segment and the N-terminal part of the M1–P1 loop, and lacks the P domains and the other TMS that are found in the complete channel TRAAK.

Distribution of TRAAK in the mouse

TRAAK expression was examined in adult mouse tissues by Northern blot. The TRAAK probe detected several transcripts with estimated sizes of 1.8, 3.4 and 7.5–9.5 kb in the brain (Figure 3A). The transcript of 1.8 kb is of approximately the same size as the cloned cDNAs. The other transcripts (3.4 and 7.5–9.5 kb) may result from usage of alternative polyadenylation signals in the 3′ non-coding sequence or may correspond to immature or alternatively spliced forms. TRAAK is expressed in brain but not in heart, skeletal muscle, liver, lung, kidney and testis. RT–PCR experiments on a larger collection of mouse tissues gave the same kind of results. In this case, TRAAK mRNA was found in the brain and also in the spinal cord and the eyes (Figure 3B). In these tissues, transcripts encoding the complete TRAAK and the truncated form TRAAKt were both amplified by using the same set of primers flanking the deletion. Respective levels of expression for both forms were quantified and found to be nearly identical (data not shown).

The regional distribution of TRAAK transcripts was

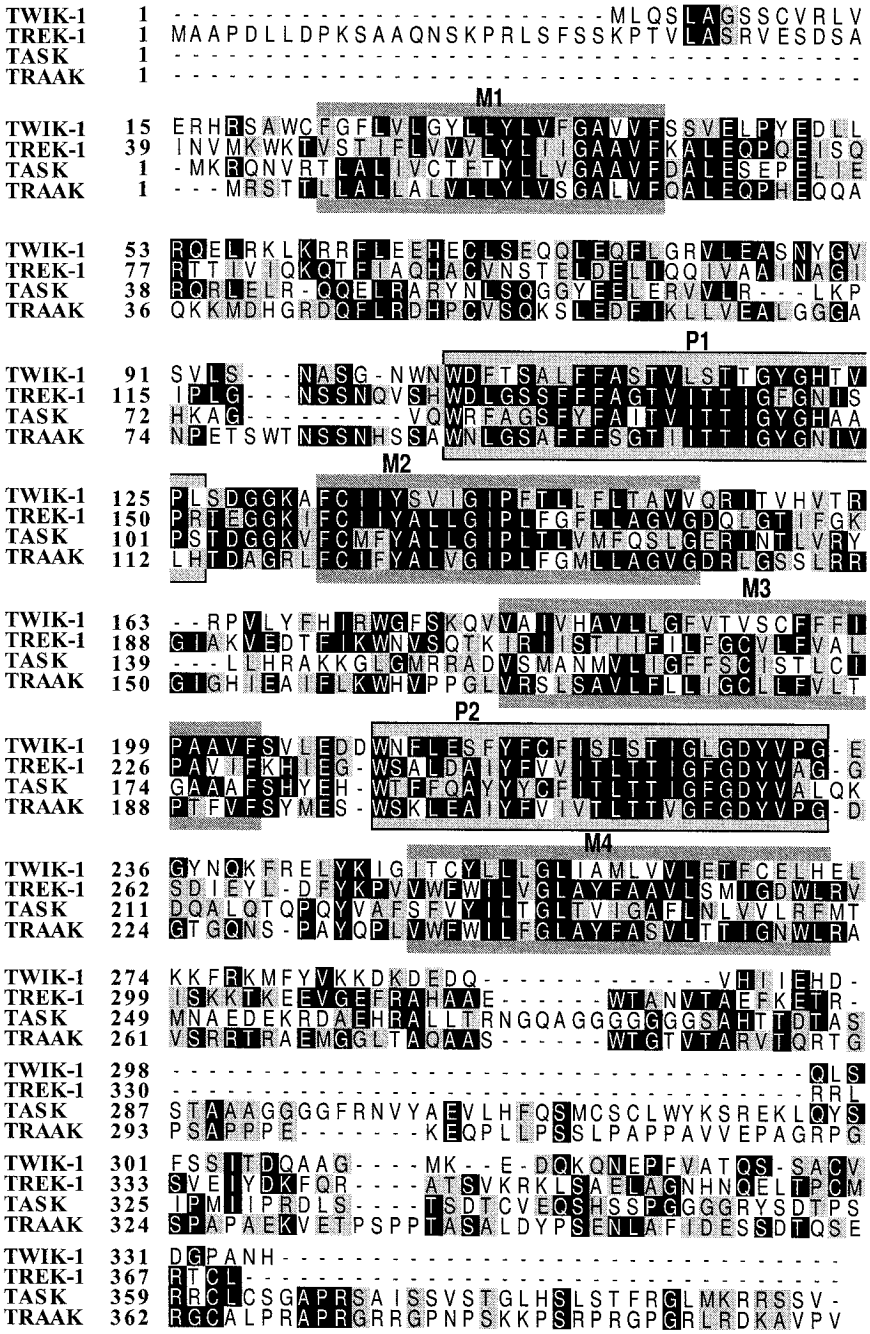
TWIK-1 1 - MLQSLAGSSCVRLV
TREK-1 1 MAAPDLLDPKSAAQNSKPRLSFSSKPTVLASRVESDSA
TASK 1 - - - - - - - - - - - - - - - - - - -

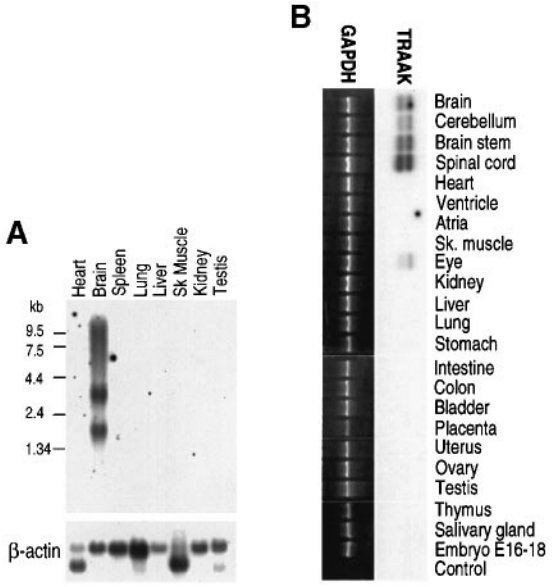

Fig. 3. Tissue distribution of TRAAK transcripts in the mouse. (**A**) A multiple tissue Northern blot from Clontech was probed at high stringency with a TRAAK cDNA probe and reprobed with a β-actin probe as a control. Each lane contains 2 μg of poly(A)$^+$ RNA. Autoradiograms were exposed for 6 days at –70°C. sk. muscle, skeletal muscle. (**B**) Tissue distribution analysis of TRAAK mRNAs by RT–PCR. Two bands are detected that correspond to the splice variants TRAAK and TRAAKt.

radiatum of all subfields were highly labeled (Figure 4E). TRAAK is also expressed in additional structures of the telencephalon, including the subiculum, the enthorinal cortex, the amygdala and the amygdalohippocampal area. The basal ganglia (caudate-putamen) displayed an intense hybridization signal (Figure 4F). In the cerebellar cortex (Figure 4G and H), the most intense labeling was detected in the Purkinje and granule cell layers. The molecular layer was labeled weakly except for a few strongly positive cells that are scattered in the cerebellar molecular layer and may correspond to stellate cells and/or basket cells. Deep cerebellar nuclei express moderate to low levels of TRAAK mRNAs. A low expression was observed over most other regions including the substantia nigra, thalamus, hypothalamus and brainstem (pons and medulla). TRAAK mRNAs in coronal sections of several subregions of the spinal cord (cervical, sacral and lumbar) are located predominantly in the gray matter in the laminae of both the dorsal and ventral horns, which include cell bodies of sensory and motor neurons, respectively (Figure 4B and I). TRAAK transcripts are also expressed intensely in the retina, with a distinct stratification pattern. The highest labeling was observed in the inner nuclear layer, composed of nuclei of Müller cells and amacrine, bipolar and horizontal neurons, in the retinal ganglion cell layer and in the photoreceptor inner segments (Figure 4J). A moderate expression of TRAAK transcripts is present in the outer nuclear layer.

TRAAK expression in Xenopus oocytes

Sequences coding for TRAAK and TRAAKt were subcloned into pEXO, a plasmid for expression in *Xenopus* oocytes. Complementary RNAs were synthesized *in vitro* then injected into oocytes. At 48 h after the injection, instantaneous and non-inactivating currents (Figure 5A) were recorded from TRAAK-expressing oocytes that were not present in uninjected oocytes (data not shown). Current–voltage (I–V) relationships of TRAAK are outwardly rectifying, and almost no inward currents were recorded in the ND96 external medium containing 2 mM K^+ (Figure 5B). However, inward currents were revealed when the external K^+ concentration ($[K^+]_{out}$) was increased to 74 mM K^+ (Figure 5A). Figure 5B presents the I–V relationships of the TRAAK current in K^+ solutions ranging from 2 to 74 mM. The experimental data fit with the Goldman–Hodgkin–Katz current equations at the different $[K^+]_{out}$ concentrations. The fitted pemeability was 0.6 ± 0.07 (n = 24) and the calculated internal K^+ concentration was 131.6 ± 7.4 mM (n = 24). This indicates that TRAAK currents show no rectification other than that predicted from the constant field assumptions. The relationship between the reversal potential and $[K^+]_{out}$ was close to the predicted Nernst value (48.7 ± 0.7 mV/decade, n = 4) (Figure 5C) and there is no sensitivity of TRAAK current reversal potential to the external Na^+ concentration from 0 to 96 mM (n = 6), as expected for a highly selective K^+ channel. We have shown previously that cell membranes of oocytes expressing the two P domain K^+ channels TWIK-1, TREK-1 or TASK channels are more polarized than control oocytes, the resting membrane potential (E_m) reaching a value close to the K^+ equilibrium potential (E_K). In oocytes expressing TRAAK, E_m was –88.2 ± 1.4 mV (n = 23, in standard ND96) instead of –43 ± 2.4 mV (n = 7) in non-injected oocytes (data not shown). This result demonstrates that TRAAK activity, as for TWIK-1, TREK-1 and TASK channels, is able to drive E_m close to E_K. No currents were recorded in the TRAAKt-expressing oocytes (0.2 ± 0.03 μA at +30 mV, n = 8).

The effects of various pharmacological agents were studied on TRAAK currents elicited by voltage pulses to +50 mV (data not shown). Currents were partially sensitive to Ba^{2+} but only at high concentrations (56.7 ± 4.6% of inhibition at +30 mV, 1 mM Ba^{2+}, n = 5) and insensitive to the other classical K^+ channels blockers such as tetraethylammonium (TEA, 1 mM), 4-aminopyridine (4AP, 1 mM) and Cs^+ (1 mM). TRAAK currents were insensitive to charybdotoxin (20 nM) and dendrotoxin (100 nM). Neither the class III antiarrhythmic tedisamil (10 μM) nor the K_{ATP} channel blockers glibenclamide (200 μM) or tolbutamide (100 μM), or the K_{ATP} channel openers pinacidil (100 μM) and P1060 (10 μM), were effective. Other ion channel blockers such as tetrodotoxin (TTX, 1 μM) or Co^{2+} (500 μM) were also without effect. The activity of the other two P domain K^+ channels TWIK-1, TREK-1 and TASK has been shown to be regulated by one or several of the following treatments: internal or external pH variations or application of agents that activate PKC or PKA. This does not seem to be the case for TRAAK, at least in the *Xenopus* oocyte system. TRAAK currents were insensitive to internal Ca^{2+} changes obtained by injection of inositol trisphosphate (IP_3, 10 mM) or EGTA (100 mM) to treatments that increase cAMP such as perfusion of IBMX (1 mM) and forskolin (10 μM), or to activation of PKC by application of the phorbol

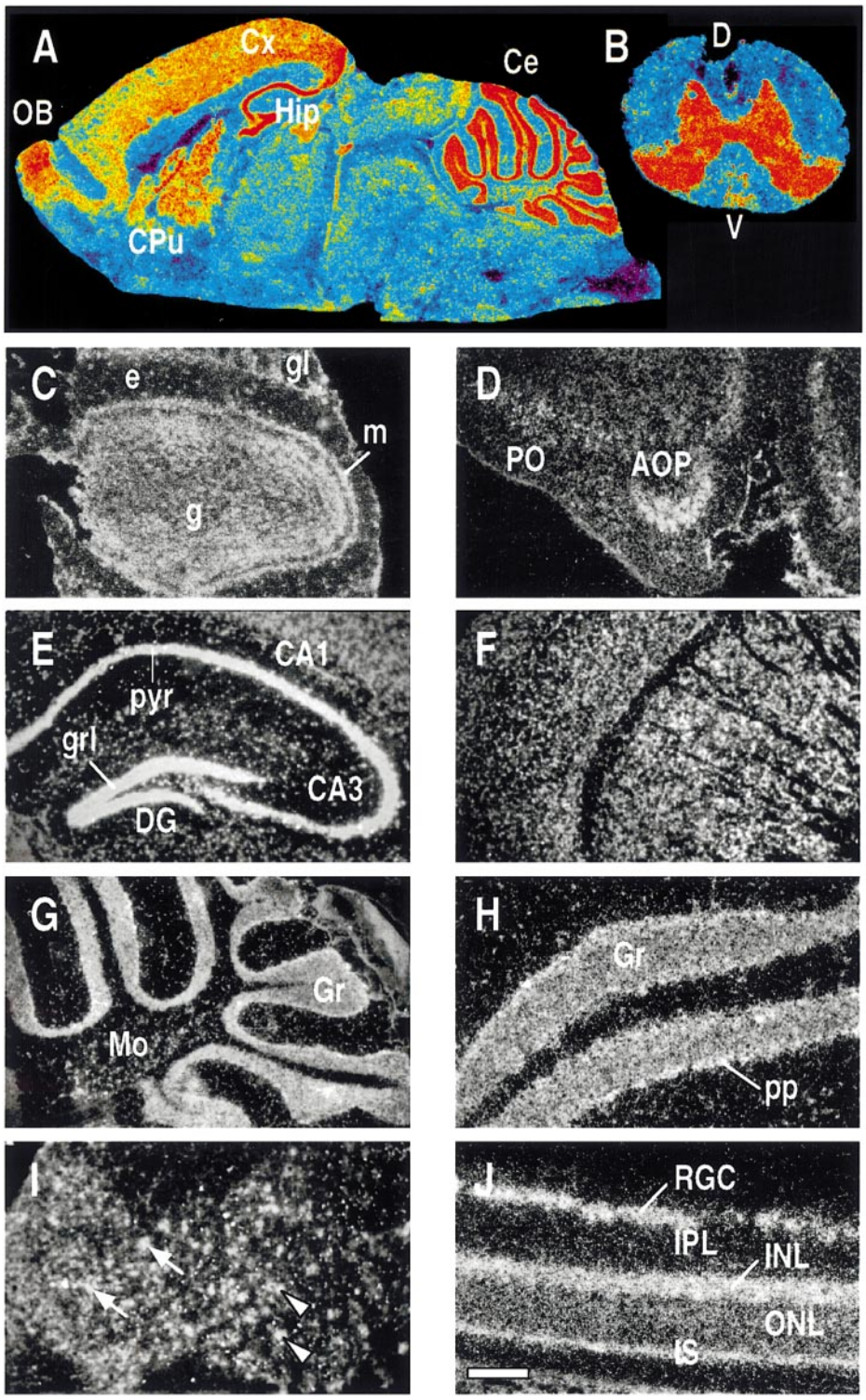

Fig. 4. TRAAK mRNA distribution in brain, spinal cord and retina of adult mouse obtained by *in situ* hybridization. (A and B) Autoradiograph showing the distribution of TRAAK transcripts in a parasagittal section of mouse brain (**A**) and spinal cord (**B**). CA1–CA3, fields CA1–CA3 of Ammon's horn; Ce, cerebellum; Cx, cerebral cortex, CPu, caudate putamen; DG, dentate gyrus; Hip, hippocampus; OB, olfactory bulb. (C–H) Dark-field photomicrographs showing the cellular localization of TRAAK mRNA in selected brain areas on emulsion-dipped sections. (**C**) Low-power magnification of a section showing the olfactory bulb: g, internal granule cell layer; m, mitral cell layer; e, external plexiform layer; gl, glomerular layer. Scale bar: 150 μm. (**D**) High magnification of a section showing the anterior olfactory nucleus (AOP) and the primary olfactory cortex (PO). Scale bar: 300 μm. (**E**) Dark-field photomicrograph of the hippocampal formation: grl, dentate granule cell layer; pyr, pyramidal layer of the CA1–CA3 fields of Ammon's horn. Scale bar: 250 μm. (**F**) Dark-field photomicrograph of the striatal region. Scale bar: 400 μm. (**G** and **H**) Low and high magnification of a section showing the cerebellum: Gr, granule cell layer; Mo, molecular cell layer; pp, Purkinje cell layer. Scale bars: (G) 150 μm; (H) 400 μm. (**I**) Dark-field photomicrograph of the ventral and dorsal horns of the lumbar spinal chord showing an intense hybridization signal on cell bodies of motoneurons (arrows) and sensory neurons (arrowheads). Scale bar: 250 μm. (**J**) Dark-field photomicrograph of a vertical section of rat retina: INL and ONL, inner and outer nuclear layers; IPL, inner plexiform layer; IS, photoreceptor inner segment; RGC, retinal ganglion cell layer. Scale bar: 400 μm.

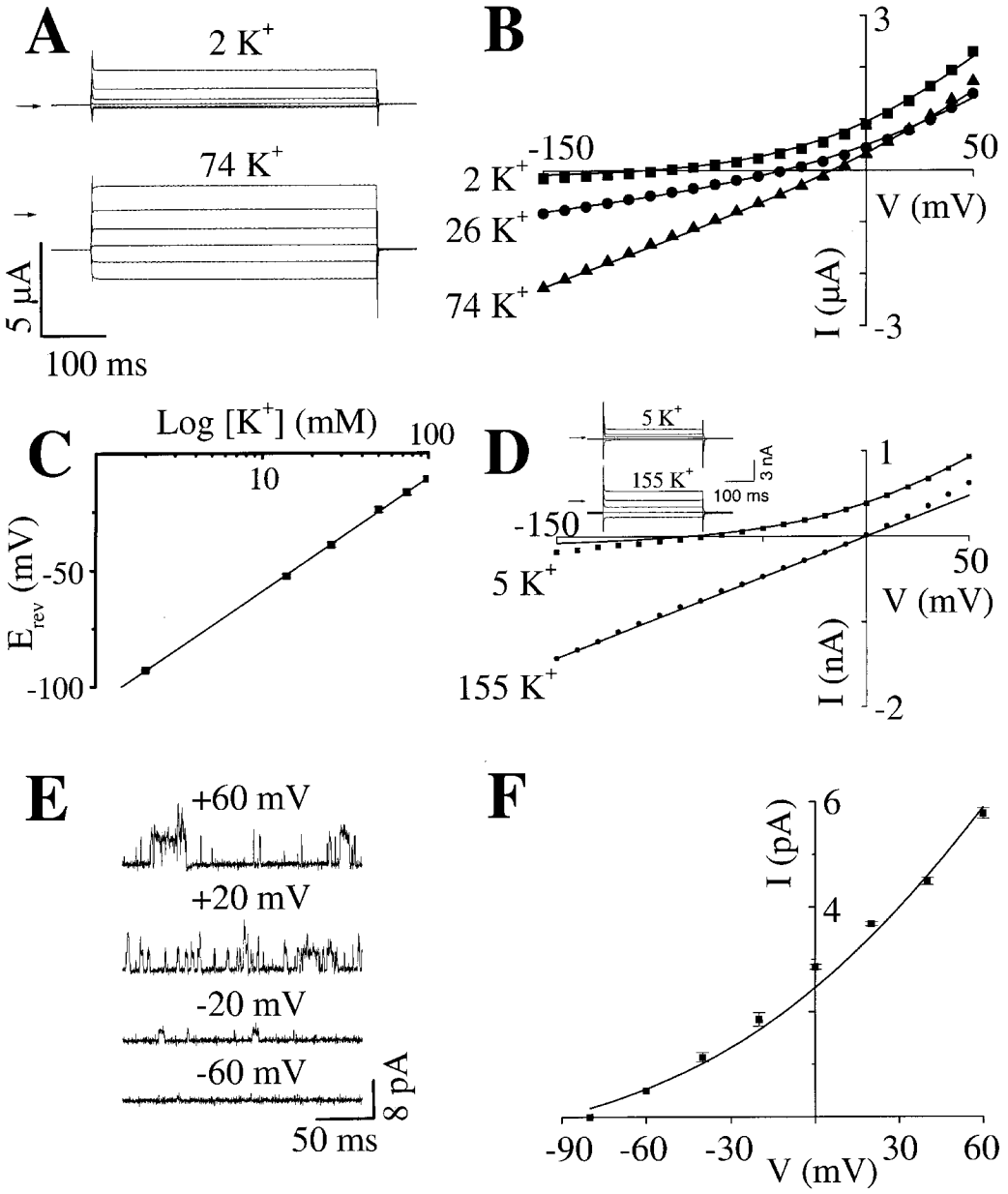

Fig. 5. Biophysical properties of TRAAK in oocytes (A–C) and COS cells (D–F). (**A**) Currents elicited by voltage pulses from –150 to +50 mV in 40 mV steps, 500 ms in duration, from a holding potential of –80 mV, in low (2 mM K^+) or high K^+ solutions (74 mM K^+). The zero current level is indicated by an arrow. (**B**) Current–voltage relationships. Mean currents were measured over the last 50 ms at the end of voltage pulses as in (A), from –150 to +50 mV, in 10 mV steps. Data (points) are fitted with the Goldman–Hodgkin–Katz current equation (lines). Modified ND96 solutions containing 2 mM KCl and 96 mM tetramethylammonium-chloride (TMA Cl) were used. TMA Cl was substituted by KCl to obtain solutions ranging from 2 to 74 mM K^+. (**C**) Reversal potential of TRAAK currents as a function of $[K^+]_{out}$ (mean ± SEM, $n = 3$). (**D**) Current–voltage relationships of mean currents measured over the last 50 ms at the end of voltage pulses as in the inset, ranging from –150 to +50 mV in 10 mV steps. K^+ solutions were prepared as in (B). Inset: TRAAK currents recorded from a transiently transfected COS cell and elicited by voltage pulses from –150 to +50 mV in 50 mV steps, 500 ms in duration, from a holding potential of –80 mV, in low (5 mM K^+) or high K^+ solutions (155 mM K^+). The zero current level is indicated by an arrow. (**E**) Single channel currents recorded in the inside-out configuration under voltage clamp at –60, –20, +20 and +60 mV. (**F**) Single channel current–voltage relationship measured during voltage clamp as in (E), ranging from –90 to +60 mV, in 20 mV steps ($n = 8$).

ester PMA (40 nM). TRAAK currents were also insensitive to an external acidification obtained by perfusion of solutions at pH 5.4 or to internal and external acidifications obtained by perfusing a solution bubbled with CO_2. In transfected COS cells (see below), a slight increase in the control current (1.0 ± 0.1 nA, $n = 6$, pH 7.3) was observed upon alkalinization at pH 9.7 (1.8 ± 0.2 nA, $n = 6$).

Activation of TRAAK by unsaturated fatty acids in COS cells

The sequence coding for TRAAK was subcloned into pIRES-CD8 under the control of the cytomegalovirus promoter to give pIREScd8–TRAAK. The RNA produced from this plasmid is polycistronic, with the sequence coding for TRAAK upstream of an internal ribosome entry site (IRES) and the sequence coding for the CD8

cell surface marker. COS cells were transiently transfected with pIREScd8–TRAAK, and cells expressing TRAAK were identified 24–48 h later by application of anti-CD8 antiboby-coated beads. The inset of Figure 5D shows whole cell currents recorded in transfected COS cells in external solutions containing 5 and 155 mM K^+. TRAAK currents were instantaneous and non-inactivating as in *Xenopus* oocytes. Mock-transfected cells did not express this K^+ channel activity (data not shown). Figure 5D presents the I–V relationships of TRAAK current in 5 and 155 mM external K^+ concentrations. Experimental data were well fitted with the Goldman–Hodgkin–Katz current equation. This demonstrates that TRAAK in COS cells has the same biophysical properties as in *Xenopus* oocytes. Inside-out patch recordings shown in Figure 5E indicate a flickering behavior for TRAAK channels. The single channel I–V relationship obtained in inside-out patches is shown in Figure 5F. The slope conductance measured between 0 and +60 mV is 45.5 ± 3.7 pS (n = 10).

Neuronal background K^+ currents (i.e. instantaneous, non-inactivating and with no voltage-dependent activation threshold) have been shown to be stimulated by AA (Premkumar *et al.*, 1990b; Kim *et al.*, 1995). TRAAK currents recorded before and after perfusion with 10 μM AA are shown in Figure 6A. A drastic stimulation of the current was observed, with no modification of the current kinetics. Current–potential relationships are presented in Figure 6B and show that stimulation of TRAAK by AA is reversible within 5 min and observed at all potentials, an inwardly directed current being obtained at hyperpolarized potentials. The concentration dependence of the AA effect on TRAAK current is shown in Figure 6C. Activation was not prevented when the AA perfusion was supplemented with a mixture of inhibitors of the AA metabolism pathway including nordihydroguaiaretic acid for lipoxygenase, indomethacin for cyclooxygenase, clotrimazole for epoxygenase, and 5,8,11,14-eicosatetraynoic acid (ETYA), an inhibitor of all three pathways (all at 10 μM)). Under these conditions, the current increase induced by AA was 6.6 ± 0.5-fold (n = 3) (at +50 mV). This result alone demonstrates that AA itself can directly stimulate TRAAK and that stimulation does not require the production of another active eicosanoid. Moreover, five of the possible eicosanoid metabolites of AA, namely 5S-, 12S- and 15S-hydroperoxyeicosatetraenoic acids (HPETE) (1 μM), and 11-12 and 14,15 epoxyeicosatrienoic acids (EET) (3 μM), were tested and were found to be inactive on TRAAK.

Neuronal AA-stimulated K^+ channels are also stimulated by other unsaturated FAs but not by saturated FAs (Kim *et al.*, 1995). We tested these same FAs on TRAAK activity. Saturated FAs palmitate (16 carbons, C16), stearate (C18) and arachidate (C20) were ineffective (at 10 μM) on TRAAK currents (Figure 6E). Conversely, the monounsaturated FA oleate (C18 Δ9) and the polyunsaturated linoleate (C18 Δ9,12), linolenate (C18 Δ9,12,15), eicosapentaenoate (EPA, C20 Δ5,8,11,14,17) and docosahexaenoate (DOHA, C20 Δ4,7,10,13,16,19) all strongly stimulated TRAAK currents (at 10 μM) (Figure 6E). Interestingly, derivatives of active FAs AA and DOHA, where the carboxyl function is substituted with an alcohol (AA-OH) or a methyl ester function (AA-ME and DOHA-ME), have no stimulation properties (Figure 6E). The reversible effect of AA on TRAAK was observed in inside-out patches (Figure 6D) but it was also recorded in outside-out patches (data not shown). These results indicate that the effects of polyunsaturated FAs on TRAAK are probably direct, via binding either to the protein itself or to its immediate lipid environment, and that additional intracellular components are not needed.

Finally, riluzole, a neuroprotective drug with anticonvulsive and anti-ischemic properties (Malgouris *et al.*, 1989; Romettino *et al.*, 1991; Stutzmann *et al.*, 1991; Pratt *et al.*, 1992; Bryson *et al.*, 1996), was also tested on TRAAK. Riluzole was found to increase TRAAK (3.9 ± 0.5-fold, n = 6) in transfected COS cells (Figure 6F).

Discussion

An increasing family of two P domain K^+ channels in mammals

TRAAK is a novel member of the extending family of TWIK-related K^+ channels (Lesage and Lazdunski, 1998). These channels have been conserved throughout evolution, and similar proteins with four TMS and two P domains are found in plants (Czempinski *et al.*, 1997), in *Drosophila* (Goldstein *et al.*, 1996) and in the nematode *Caenorhabditis elegans*, where >39 genes potentially encoding such proteins have now been identified (Salkoff *et al.*, 1997). With this new TRAAK channel, four different K^+ channels of this family have now been isolated in mammals (Fink *et al.*, 1996; Lesage *et al.*, 1996a, 1997; Duprat *et al.*, 1997; Leonoudakis *et al.*, 1998). Despite the same topology, amino acid conservation is relatively low between these proteins (25–38% identity). TRAAK displays an electrophysiological behavior more related to that of TASK (Duprat *et al.*, 1997; Leonoudakis *et al.*, 1998) than to other members of the family (Fink *et al.*, 1996; Lesage *et al.*, 1996a, 1997). The outward rectification of both TRAAK and TASK can be approximated by the Goldman–Hodgkin–Katz current equation that predicts a curvature of the I–V plot in asymmetric K^+ conditions. This suggests that TRAAK, like TASK, lacks intrinsic voltage sensitivity. The absence of apparent activation and inactivation kinetics as well as voltage independence are characteristic of conductances referred to as background conductances (Siegelbaum *et al.*, 1982; Yue and Marban, 1988; Pellegrini *et al.*, 1989; Premkumar *et al.*, 1990a,b; Koh *et al.*, 1992; Koyano *et al.*, 1992; Shen *et al.*, 1992; Backx and Marban, 1993; Wu *et al.*, 1993; Enyeart *et al.*, 1996; Theander *et al.*, 1996; Buckler, 1997; Wagner and Dekin, 1997).

A peculiarity of TRAAK is the existence of an intriguing truncated splice variant called TRAAKt. This variant is probably produced by the deletion of one exon. This deletion introduces a frameshift in the coding sequence that results in the formation of a premature stop codon. The predicted product consists of a single TMS corresponding to M1 and a C-terminus corresponding to the proximal part of the M1–P1 interdomain. Transcripts for both truncated and complete forms are expressed at approximately the same level in tissues expressing TRAAK. This suggests that both TRAAK products could have an important physiological role. However, the exact function of TRAAKt remains to be elucidated since, not surprisingly, this structure which lacks the conventional P domains is also unable to generate K^+ currents.

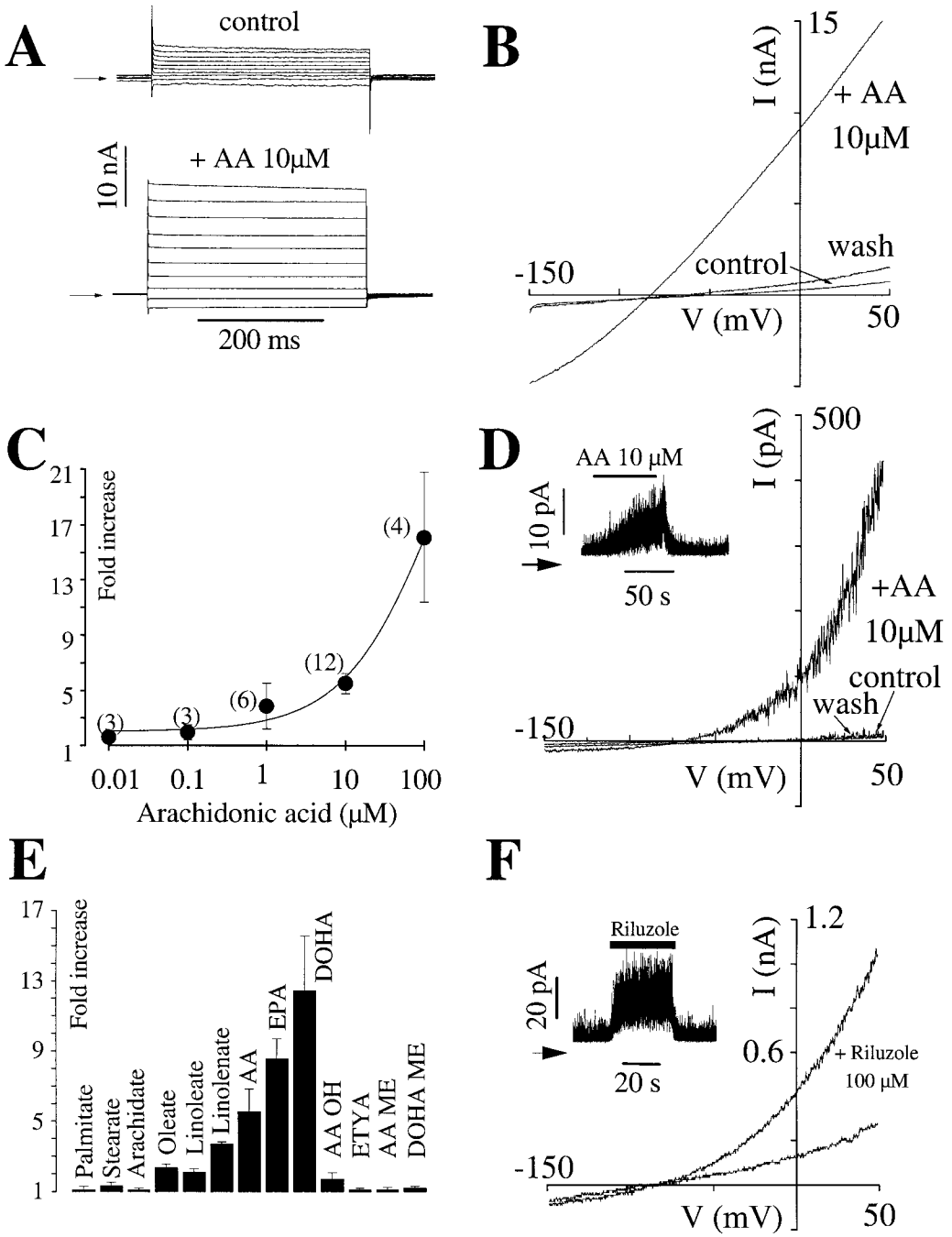

Fig. 6. Fatty acid activation of TRAAK in COS cells. (**A**) The whole-cell configuration of the patch–clamp technique was used with COS cells transfected with TRAAK. Currents elicited by voltage pulses ranging from –130 to +50 mV in 20 mV steps, 600 ms in duration from a holding potential of –80 mV, before (control) and after 2 min perfusion with 10 μM AA. The zero current level is indicated by an arrow. (**B**) Current–voltage relationships obtained with voltage ramps ranging from –150 to +50 mV, 500 ms in duration, before (control), after 3 min perfusion with 10 μM AA and after the wash. (**C**) Dose dependence of TRAAK activation by AA; the fold increase (measured current at +50 mV after 3 min exposure relative to the current recorded before exposure) is plotted against the AA concentration in μM (mean ± SEM, number of tested cells in parentheses). (**D**) Current–voltage relationships obtained in an inside-out patch with voltage ramps ranging from –150 to +50 mV, 500 ms in duration, before (control), after 3 min perfusion with 10 μM AA and after the wash. Inset: effects of 10 μM AA on TRAAK currents recorded in an inside-out patch clamped at +20 mV. The zero current level is indicated by an arrow. (**E**) Bar graphs of the fold increase (measured current at +50 mV after 3 min exposure relative to the current recorded before exposure) after perfusion with various FAs. In all cases, the effects of FAs have been measured when the maximum activation was obtained, or 3 min after perfusion for non-active FAs. (**F**) Effect of riluzole on TRAAK current. Current–voltage relationships were obtained as in (D) before and after application of riluzole (100 μM). Insets: effect of riluzole at +40 mV on outside-out patches.

TRAAK, a fatty acid-stimulated K^+ channel

AA modulation of K^+ channels is widespread and diverse because both inhibitory and stimulatory phenomena can be observed (Meves, 1994). An inhibitory effect of AA on different cloned and native K^+ channels in brain has been reported (Villarroel, 1993; Honoré *et al.*, 1994; Villarroel and Schwarz, 1996; Keros and McBain, 1997). However, AA has also been shown to stimulate a particular

class of K^+ channels in neuronal cells (Premkumar *et al.*, 1990b; Kim *et al.*, 1995). These channels are stimulated not only by AA but more generally by unsaturated FAs, while saturated FAs are without effect (Kim *et al.*, 1995).

We demonstrate here that TRAAK currents are also strongly stimulated by AA. This stimulation is reversible, concentration-dependent and direct (i.e. not via kinase C activation). Not only AA but also other polyunsaturated FAs enhance TRAAK currents while saturated FAs are without effect. Native AA-stimulated K^+ currents that have been described in neurons from mesencephalic and hypothalamic areas of rat brain are highly similar to TRAAK in terms of both electrophysiological behavior and pharmacological properties (Kim *et al.*, 1995). They are instantaneous and outward rectifying in normal external K^+ and they have a unitary conductance of 45 pS. They are partially inhibited by Ba^{2+} at high concentrations (2 mM) and they are insensitive to TEA and 4-AP, as is TRAAK. We propose that TRAAK, which is the first molecularly identified FA-stimulated K^+ channel, is an essential component of these neuronal AA-stimulated channels.

Biological significance of TRAAK stimulation

Depending on the levels at which it is produced, AA can have both important physiological and pathophysiological effects. For example, it has been suggested that AA is involved in presynaptic inhibition of sensory neurons (Piomelli *et al.*, 1987) and in synaptic depression in the striatum (Piomelli *et al.*, 1991; Calabresi *et al.*, 1992). In the first case, an AA-stimulated background K^+ channel has been clearly implicated. AA could also act as a retrograde messenger to control synaptic transmission (Kandell and O'Dell, 1992; Bliss and Collingridge, 1993). All these effects may well be related to the capacity of AA to stimulate the TRAAK channel. On the other hand, AA release is markedly enhanced in pathophysiological conditions such as seizures, experimentally induced convulsions or brain ischemia (Burton *et al.*, 1986), and this excess AA liberation is thought to be highly deleterious for neuronal cells (Bazan, 1989; Chan *et al.*, 1989; Siesjö *et al.*, 1989). Finally, the many hormones, neurotransmitters, growth factors and cytokines that evoke receptor-dependent hydrolysis of AA-containing phospholipids and the multiple consequences of AA-induced K^+ channel stimulation in the brain also make it possible that this class of channel proteins is involved in diverse human disease states. At low concentrations (0.1–1 μM), AA will stimulate the TRAAK channel by factors of 2–4 and this will be ample to produce physiological hyperpolarizations. At high concentrations (10–100 μM), AA will increase TRAAK activity by factors of 6–16. The effect will be expected to be protective in the first place because it also produces a hyperpolarization, but this hyperpolarization will not last because potent opening of these TRAAK channels will probably gradually tend to empty neurons of their internal K^+ content. A decrease in the internal K^+ concentration associated with an increase in the extracellular K^+ will then very rapidly be deleterious to the central nervous system (Hansen, 1985; Siesjö and Wieloch, 1985).

Levels of FAs are controlled by agonist-stimulated and basal phospholipase activities. However, they also vary with changes in the metabolism of unesterified FAs and fluctuations in extracellular sources of FAs due to nutritional and hormone states and tissue injury. Thus, the potential regulatory roles of FAs in the control of K^+ channels range from that of a lipid-derived second messenger to a signal carried via circulation. The identification of the AA-stimulated K^+ channel TRAAK provides molecular probes to better understand the physiological function of this class of K^+ channels as well as a defined target for the development of new therapeutic agents. Opening of other classes of K^+ channels such as ATP-sensitive K^+ channels (K_{ATP}) is known to lead to potent protection against both cardiac and brain ischemia (Quast, 1992; Heurteaux *et al.*, 1993; Quast and Weston, 1994). However, activators of K_{ATP} channels are not yet used in clinical practice for this purpose. Riluzole, which is a potent neuroprotective drug with anticonvulsive and anti-ischemic properties (Malgouris *et al.*, 1989; Romettino *et al.*, 1991; Stutzmann *et al.*, 1991; Pratt *et al.*, 1992), is currently used to prolong survival of patients with amyotrophic lateral sclerosis (ALS) (Bensimon *et al.*, 1994; Bryson *et al.*, 1996). Riluzole was found to increase TRAAK activity by a factor of four. Thus, riluzole might exert at least part of its beneficial effects through stimulation of this peculiar class of K^+ channels.

Materials and methods

Cloning of TRAAK

The sequence of TREK-1 was used to search homologs in public DNA databases by using the tBLASTn alignment program (Altschul *et al.*, 1990), and led to the isolation of an EST (DDBJ/EMBL/GenBank accession No. AA155263) which showed significant similarities with TREK-1, TWIK-1 and TASK. Two oligonucleotides were designed from this EST: sense strand, 5′-CGGGATCCTTCTCTGAGTCTTCTGAC-3′; and antisense strand, 5′-CGGAATTCCAGGCTCTTCTGGC-3′, introducing *Bam*HI and *Eco*RI sites, respectively. They were used to amplify a 330 bp fragment from mouse brain poly(A)$^+$-derived cDNAs and subcloned into pBluescriptII SK$^-$ (Stratagene). This fragment was sequenced, ^{32}P-labeled and used to screen a mouse brain cDNA library as previously described (Fink *et al.*, 1996). From 5×10^5 phages screened, two independent positive clones were obtained. The longer one was excised from λZAPII XR vector into pBluescriptII SK$^-$. The cDNA insert was characterized by restriction analysis and by complete sequencing on both strands using the dideoxynucleotide termination method and an automatic sequencer (Applied Biosystem, model 373A). This clone (1.6 kb) was shown to contain a short ORF encoding a 67 amino acid polypeptide. Sequence comparison with other TWIK-related K^+ channels showed a good similarity up to the M1–P1 extracellular linker loop. By translating the nucleic acid sequence in other frames, good similarity was recovered with the corresponding TMS (M2, M3 and M4) and P domains (P1 and P2) of TREK-1. This suggested that this cDNA was a natural truncated form derived from a deletion in a longer ORF, and was called TRAAKt. This hypothesis was verified by RT–PCR experiments on mouse brain cDNA. A set of specific primers was designed upstream and downstream of the predicted deleted region and led to the amplification of two populations of fragments. These fragments were sequenced from two different amplification experiments in order to exclude sequence errors due to the PCR technique. Their sequencing revealed that the shorter fragment encoded TRAAKt and the longer, called TRAAK, contained a new ORF with an additional sequence of 127 nucleotides. The entire coding sequence of mouse TRAAK was obtained by PCR amplification with a low error rate DNA polymerase (Pwo DNA polymerase, Boehringer Mannheim) on mouse brain cDNA using a set of specific primers, verified by complete sequencing and subcloned into pBluescriptII SK$^-$ to give pBS-TRAAK.

Analysis of TRAAK mRNA distribution

For Northern blot analysis, a mouse Multiple Tissue Northern (MTN) blot was purchased from Clontech and hybridized at 65°C in ExpressHyb

solution with an *Eco*RI–*Xho*I ^{32}P-labeled fragment from pBS-TRAAK following the manufacturer's protocol. For RT–PCR, total RNAs were extracted from mouse tissues with the SNAP total RNA isolation kit (Invitrogen) and treated with DNase. Fifteen μg of total RNA were reverse-transcribed according to the manufacturer's instructions (Gibco-BRL) and 1/40 of each sample was used as template for PCR amplification (*Taq* DNA polymerase, Gibco-BRL) using mouse TRAAK (base positions 409–426: 5′- CCGAGACCAGTTTCTGAG-3′ and 908–926: 5′-CTACAGTGGTGAGAGTCAC-3′) and GAPDH (Clontech) primers. TRAAK amplified fragments were transferred onto nylon membranes then probed with a ^{32}P-labeled internal primer (bases 645–664: 5′-GTATCTTCTATGCACTGGTG-3′).

In situ hybridization experiments were performed on adult Swiss mice using standard procedures. The dissected organs (brains, spinal cords, retinas) were fixed in ice-cold 4% (w/v) paraformaldehyde/0.1 M sodium phosphate buffer solution (PBS, pH 7.4) for 2 h and then immersed overnight at 4°C in a 20% sucrose/PBS solution. Frozen sections (10 μm) were cut on a cryostat (Leica) at –25°C, collected on 3-aminopropyl-ethoxysilane-coated slides and stored at –20°C until use. Specific antisense cRNA probes were generated with T3 RNA polymerase (Boehringer Mannheim), by *in vitro* transcription using [α-^{33}P]UTP (3000 Ci/mmol, ICN Radiochemicals), from *Nhe*I-linearized plasmid containing a 600 bp fragment of TRAAK cDNA in the 3′-untranslated sequence, inserted into pEXO. Sections were treated consecutively with 0.1 M glycine in PBS for 10 min, PBS for 3 min, 5 μg/ml of proteinase K diluted in 0.1 M Tris/50 mM EDTA (pH 8.0) for 15 min at 37°C and 4% paraformaldehyde/PBS (pH 7.2) for 5 min. Slides were then rinsed for 10 min in PBS, acetylated for 10 min in 0.25% acetic anhydride in 0.1 M triethanolamine and dehydrated. Hybridization was carried out overnight at 65°C in hybridization buffer (50% deionized formamide, 10% dextran sulfate, 500 μg/ml denatured salmon sperm DNA, 1% Denhardt's, 5% Sarkosyl, 250 μg/ml yeast tRNA, 20 mM dithiothreitol, 20 mM $NaPO_4$ in 2× SSC and the radiolabeled probe (at 0.2 ng/ml with specific activities of 8×10^8 d.p.m./mg). Following hybridization, sections were washed in 4× SSC for 15 min and then twice in 1× SSC for 30 min at 60°C, treated with RNase A (5 μg/ml) in 2× SSC for 15 min at 37°C, and washed twice with 1× SSC for 30 min, followed by two 15 min washes in 0.1× SSC at 30°C. Specimens were then dehydrated, air-dried and exposed to Amersham β-max Hyperfilm for 5 days at 4°C. Selected slides were dipped in Amersham LM1 photographic emulsion and exposed for 3 weeks at 4°C and then developed in Kodak D-19 for 4 min. All slides were counterstained with hematoxylin/eosin. For control experiments, adjacent sections were hybridized with the corresponding sense riboprobe or digested with RNase before hybridization.

Electrophysiological measurements in Xenopus oocytes

The sequences coding for TRAAK and TRAAKt were subcloned into the pEXO vector (Lingueglia *et al.*, 1993) to give pEXO–TRAAK and pEXO–TRAAKt, respectively. Capped cRNAs were synthesized *in vitro* from the linearized plasmids by using the T7 RNA polymerase (Stratagene). *Xenopus laevis* were purchased from CRBM (Montpellier, France). Preparation and cRNA injection of oocytes has been described elsewhere (Guillemare *et al.*, 1992). Oocytes were used for electrophysiological studies 2–4 days following injection (20 ng/oocyte). In a 0.3 ml perfusion chamber, a single oocyte was impaled with two standard microelectrodes (1–2.5 MΩ resistance) filled with 3 M KCl and maintained under voltage clamp by using a Dagan TEV 200 amplifier, in standard ND96 solution (96 mM NaCl, 2 mM KCl, 1.8 mM $CaCl_2$, 2 mM $MgCl_2$, 5 mM HEPES pH 7.4 with NaOH). Stimulation of the preparation, data acquisition and analysis were performed using pClamp software (Axon instruments, USA). Drugs were applied externally by addition to the superfusate (flow rate: 3 ml/min) or injected intracellularly by using a pressure microinjector (Inject+Matic, Switzerland). All experiments were performed at room temperature (21–22°C).

Patch–clamp recordings in transfected COS cells

The sequence coding for TRAAK was excised from the pEXO–TRAAK construct and subcloned into pIRESneo vector (Clontech) and into pIRES-CD8 vector to give pIRESneo–TRAAK and pIREScd8–TRAAK, respectively. pIRES-CD8 vector was obtained by replacing the *neo^r* gene in the original vector by the coding sequence of the T-type lymphocyte surface marker CD8. COS cells were seeded at a density of 20 000 cells per 35 mm dishes 24 h prior transfection. Cells were then transiently transfected by the classical DEAE-dextran method with 1 μg of pIREScd8–TRAAK plasmid per 35 mm dish. Transiently transfected cells were visualized 48 h after transfection using the anti-CD8 antibody-coated beads method (Jurman *et al.*, 1994).

For whole-cell recordings, the internal solution contained 150 mM KCl, 3 mM $MgCl_2$, 5 mM EGTA and 10 mM HEPES pH 7.2 with KOH, and the external solution 150 mM NaCl, 5 mM KCl, 3 mM $MgCl_2$, 1 mM $CaCl_2$, 10 mM HEPES pH 7.4 with NaOH. For inside-out and outside-out recordings, 150 mM KCl in the internal solution and 150 mM NaCl in the external solution were substituted with 150 mM K gluconate and 150 mM Na gluconate, respectively. Because of their high oxygen sensitivity, FA (Sigma) stock solutions were prepared at 0.1 M (ethanol), flushed with N_2 and kept at –20°C for 48 h at most. The final solutions were made regularly and sonicated for 20 s prior to use.

Acknowledgements

We thank Drs J.Barhanin, E.Honoré and G.Romey for very helpful discussions, M.Jodar, N.Leroudier, N.Gomez and G.Jarretou for expert technical assistance, and Y.Benhamou for secretarial assistance. We are also very grateful to Dr A.Patel for careful reading of this manuscript. This work was supported by the Centre National de la Recherche Scientifique (CNRS) and the Association Française contre les Myopathies (AFM).

References

Altschul,S.F., Gich,W., Miller,W., Myers,E.W. and Lipman,D.J. (1990) Basic local alignment search tool. *J. Mol. Biol.*, **215**, 403–410.

Backx,P.H. and Marban,E. (1993) Background potassium current active during the plateau of the action potential in guinea-pig ventricular myocytes. *Circ. Res.*, **72**, 890–900.

Barhanin,J., Lesage,F., Guillemare,E., Fink,M., Lazdunski,M. and Romey,G. (1996) KvLQT1 and IsK (minK) proteins associate to form the IKs cardiac potassium current. *Nature*, **384**, 78–80.

Barnard,E.A. (1996) The transmitter-gated channels: a range of receptor types and structures. *Trends Pharmacol Sci.*, **17**, 305–309.

Bazan,N.G. (1989) Arachidonic acid in the modulation of excitable membrane function and at the onset of brain damage. *Ann. NY Acad. Sci.*, **559**, 1–16.

Bensimon,G., Lacomblez,L. and Meininger,V. (1994) A controlled trial of riluzole in amyotrophic lateral sclerosis. *N. Engl. J. Med.*, **330**, 585–591.

Bliss,T.V.P. and Collingridge,G.L. (1993) A synaptic model of memory: long-term potentiation in the hippocampus. *Nature*, **361**, 31–39.

Bryson,H.M., Fulton,B. and Benfield,P. (1996) Riluzole: a review of its pharmacodynamic and pharmacokinetic properties and therapeutic potential in amyotrophic lateral sclerosis. *Drug Eval.*, **52**, 549–563.

Buckler,K.J. (1997) A novel oxygen-sensitive potassium current in rat carotid body type I cells. *J. Physiol. (Lond.)*, **498**, 649–662.

Burton,K.P., Buja,L.M., Sen,A., Willerson,J.T. and Chien,K.R. (1986) Accumulation of arachidonate in triacylglycerols and unesterified fatty acids during ischemia and reflow in the isolated rat heart. *Am. J. Physiol.*, **124**, 238–245.

Calabresi,P., Maj,R., Pisani,A., Mercuri,N.B. and Bernardi,G. (1992) Long term synaptic depression in the striatum: physiological and pharmacological characterization. *J. Neurosci.*, **12**, 4224–4233.

Chan,P.H. *et al*. (1989) The role of arachidonic acid and oxygen radical metabolites in the pathogenesis of vasogenic brain edema and astrocytic swelling. *Ann. NY Acad. Sci.*, **559**, 237–247.

Czempinski,K., Zimmermann,S., Ehrhardt,T. and Müller-Rober,B. (1997) New structure and function in plant K^+ channels: KCO1, an outward rectifier with a steep Ca^{2+} dependency. *EMBO J.*, **16**, 2565–2575.

Duprat,F., Lesage,F., Fink,M., Reyes,R., Heurteaux,C. and Lazdunski,M. (1997) TASK, a human background K^+ channel to sense external pH variations near physiological pH. *EMBO J.*, **16**, 5464–5471.

Enyeart,J.J., Mlinar,B. and Enyeart,J.A. (1996) Adrenocorticotropic hormone and cAMP inhibit noninactivating K^+ current in adrenocortical cells by an A-kinase-independent mechanism requiring ATP hydrolysis. *J. Gen. Physiol.*, **108**, 251–264.

Fakler,B. and Ruppersberg,J.P. (1996) Functional and molecular diversity classifies the family of inward-rectifier K^+ channels. *Cell Physiol. Biochem.*, **6**, 195–209.

Fink,M., Duprat,F., Lesage,F., Reyes,R., Romey,G., Heurteaux,C. and Lazdunski,M. (1996) Cloning, functional expression and brain localization of a novel unconventional outward rectifier K^+ channel. *EMBO J.*, **15**, 6854–6862.

Glowatzki,E., Fakler,G., Brandle,U., Rexhausen,U., Zenner,H.P., Ruppersberg,J.P. and Fakler,B. (1995) Subunit-dependent assembly of inward-rectifier K^+ channels. *Proc. R. Soc. Lond. B Biol. Sci.*, **261**, 251–261.

Goldstein,S.A.N., Price,L.A., Rosenthal,D.N. and Pausch,M.H. (1996) ORK1, a potassium-selective leak channel with two pore domains cloned from *Drosophila melanogaster* by expression in *Saccharomyces cerevisiae*. *Proc. Natl Acad. Sci. USA*, **93**, 13256–13261.

Guillemare,E., Honore,E., Pradier,L., Lesage,F., Schweitz,H., Attali,B., Barhanin,J. and Lazdunski,M. (1992) Effects of the level of messenger RNA expression on biophysical properties, sensitivity to neurotoxins, and regulation of the brain delayed-rectifier K^+ channel Kv1.2. *Biochemistry*, **31**, 12463–12468.

Hansen,A.J. (1985) Effects of anoxia on ion distribution in the brain. *Physiol. Rev.*, **69**, 101–148.

Hartmann,H.A., Kirsch,G.E., Drewe,J.A., Taglialatela,M., Joho,R.H. and Brown,A.M. (1991) Exchange of conduction pathways between two related K^+ channels. *Science*, **251**, 942–944.

Heginbotham,L., Lu,Z., Abramson,T. and MacKinnon,R. (1994) Mutations in the K^+ channel signature sequence. *Biophys. J.*, **66**, 1061–1067.

Heurteaux,C., Bertaina,V., Widmann,C. and Lazdunski,M. (1993) K^+ channel openers prevent global ischemia-induced expression of c-*fos*, c-*jun*, heat shock protein, and amyloid β-protein precursor genes and neuronal death in rat hippocampus. *Proc. Natl Acad. Sci. USA*, **90**, 9431–9435.

Hille,B. (ed.) (1992) *Ionic Channels of Excitable Membranes.* 2nd edn. Sinauer Associates Inc., Sunderland, MA.

Honoré,E., Barhanin,J., Attali,B., Lesage,F. and Lazdunski,M. (1994) External blockade of the major cardiac delayed-rectifier K^+ channel (Kv1.5) by polyunsaturated fatty acids. *Proc. Natl Acad. Sci. USA*, **91**, 1937–1944.

Inagaki,N., Gonoi,T., Clement,J.-P., Namba,N., Inazania,J., Gonzalez,G., Aguilar-Bryan,L., Seino,S. and Bryan,J. (1995) Reconstitution of IK_{ATP}: an inward rectifier subunit plus the sulfonylurea receptor. *Science*, **270**, 1166–1169.

Isacoff,E.Y., Jan,Y.N. and Jan,L.Y. (1990) Evidence for the formation of heteromultimeric potassium channels in *Xenopus* oocytes. *Nature*, **345**, 530–534.

Isomoto,S., Kondo,C. and Kurachi,Y. (1997) Inwardly rectifying potassium channels: their molecular heterogeneity and function. *Jap. J. Physiol.*, **47**, 11–39.

Jan,L.Y. and Jan,Y.N. (1994) Potassium channels and their evolving gates. *Nature*, **371**, 119–122.

Jurman,M.E., Boland,L.M. and Yellen,G. (1994) Visual identification of individual transfected cells for electrophysiology using antibody-coated beads. *BioTechniques*, **17**, 876–881.

Kandell,E.R. and O'Dell,T.J. (1992) Are adult learning mechanisms also used for development. *Science*, **256**, 243–245.

Kemp,B.E. and Pearson,R.B. (1990) Protein kinase recognition sequence motifs. *Trends Biochem. Sci.*, **15**, 342–346.

Keros,S. and McBain,C.J. (1997) Arachidonic acid inhibits transient potassium currents and broadens action potentials during electrographic seizures in hippocampal pyramidal and inhibitory interneurons. *J. Neurosci.*, **17**, 3476–3487.

Kim,D.H., Sladek,C.D., Aguadovelasco,C. and Mathiasen,J.R. (1995) Arachidonic acid activation of a new family of K^+ channels in cultured rat neuronal cells. *J. Physiol. (Lond.)*, **484**, 643–660.

Koh,D.S., Jonas,P., Brau,M.E. and Vogel,W. (1992) A TEA-insensitive flickering potassium channel active around the resting potential in myelinated nerve. *J. Membr. Biol.*, **130**, 149–162.

Koyano,K., Tanaka,K. and Kuba,K. (1992) A patch–clamp study on the muscarine-sensitive potassium channel in bullfrog sympathetic ganglion cells. *J. Physiol. (Lond.)*, **454**, 231–246.

Kyte,J. and Doolittle,R. (1982) A simple model for displaying the hydropathic character of a protein. *J. Mol. Biol.*, **157**, 105–106.

Leonoudakis,D., Gray,A.T., Winegar,B.D., Kindler,C.H., Harada,M., Taylor,D.M., Chavez,R.A., Forsayeth,J.R. and Yost,C.S. (1998) An open rectifier potassium channel with two pore domains in tandem cloned from rat cerebellum. *J. Neurosci.*, **18**, 868–877.

Lesage,F. and Lazdunski,M. (1998) Potassium channels with two P domains. In Kurachi,Y., Jan,L.Y. and Lazdunski,M. (eds), *Potassium Ion Channels: Molecular Structure, Function and Diseases*. Academic Press, San Diego, CA, in press.

Lesage,F., Guillemare,E., Fink,M., Duprat,F., Lazdunski,M., Romey,G. and Barhanin,J. (1996a) TWIK-1, a ubiquitous human weakly inward rectifying K^+ channel with a novel structure. *EMBO J.*, **15**, 1004–1011.

Lesage,F., Reyes,R., Fink,M., Duprat,F., Guillemare,E. and Lazdunski,M. (1996b) Dimerization of TWIK-1 K^+ channel subunits via a disulfide bridge. *EMBO J.*, **15**, 6400–6407.

Lesage,F., Lauritzen,I., Duprat,F., Reyes,R., Fink,M., Heurteaux,C. and Lazdunski,M. (1997) The structure, function and distribution of the mouse TWIK-1 K^+ channel. *FEBS Lett.*, **402**, 28–32.

Lingueglia,E., Voilley,N., Waldmann,R., Lazdunski,M. and Barbry,P. (1993) Expression cloning of an epithelial amiloride-sensitive Na^+ channel—a new channel type with homologies to *Caenorhabditis elegans* degenerins. *FEBS Lett.*, **318**, 95–99.

MacKinnon,R. (1995) Pore loops: an emerging theme in ion channel structure. *Neuron*, **14**, 889–892.

Malgouris,C., Bardot,F., Daniel,M., Pellis,F., Rataud,J., Uzan,A., Blanchard,J.C. and Laduron,P.M. (1989) Riluzole, a novel antiglutamate, prevents memory loss and hippocampal neuronal damage in ischemic gerbils. *J. Neurosci.*, **9**, 3720–3727.

Meves,H. (1994) Modulation of ion channels by arachidonic acid. *Prog. Neurobiol.*, **43**, 175–186.

Nichols,C.G. and Lopatin,A.N. (1997) Inward rectifier potassium channels. *Annu. Rev. Physiol.*, **59**, 171–191.

Pellegrini,M., Simoni,A. and Pellefrino,M. (1989) Two types of K^+ channels in excised patches of somatic membrane of leech AP neuron. *Brain Res.*, **483**, 294–300.

Piomelli,D., Volterra,A., Dale,N., Siegelbaum,S.A., Kandel,E.R., Schwarz,J.H. and Belardetti,F. (1987) Lipoxygenase metabolites of arachidonic acid as second messengers for presynaptic inhibition of *Aplysia* sensory neurons. *Nature*, **328**, 38–43.

Piomelli,D., Pilon,C., Giros,B., Sokoloff,P., Martres,M.P. and Schwartz,J.C. (1991) Dopamine activation of the arachidonic acid cascade as a basis for D1/D2 receptor synergism. *Nature*, **353**, 164–167.

Pongs,O. (1992) Molecular biology of voltage-dependent potassium channels. *Physiol. Rev.*, **72**, S69–S88.

Pongs,O. (1995) Regulation of the activity of voltage-gated potassium channels by beta subunits. *Semin. Neurosci.*, **7**, 137–146.

Pratt,J., Rataud,J., Bardot,F., Roux,M., Blanchard,J.C., Laduron,P.M. and Stuzmann,J.M. (1992) Neuroprotective actions of riluzole in rodent models of global and local ischaemia. *Neurosci. Lett.*, **140**, 225–230.

Premkumar,L.S., Chung,S.H. and Gage,P.W. (1990a) GABA-induced potassium channels in cultured neurons. *Proc. R. Soc. Lond.*, **241**, 153–158.

Premkumar,L.S., Gage,P.W. and Chung,S.H. (1990b) Coupled potassium channels induced by arachidonic acid in cultured neurons. *Proc. R. Soc. Lond. B Biol. Sci.*, **242**, 17–22.

Quast,U. (1992) K^+ channel openers: pharmacological and clinical aspects. *Fund. Clin. Pharmacol.*, **6**, 279–293.

Quast,U. and Weston,A.H. (1994) Mammalian potassium channels. *Trends Pharmacol. Sci.*, **15**, 135.

Romettino,S., Lazdunski,M. and Gottesmann,C. (1991) Anticonvulsant and sleepwaking influences of riluzole in a rat model of absence epilepsy. *Eur. J. Pharmacol.*, **199**, 371–373.

Rudy,B. (1988) Diversity and ubiquity of K^+ channels. *Neuroscience*, **25**, 729–749.

Ruppersberg,J.P., Schröter,K.H., Sakman,B., Stocker,M., Sewing,S. and Pongs,O. (1990) Heteromultimeric channels formed by rat brain potassium channel protein. *Nature*, **345**, 535–537.

Salkoff,L., Butler,A., Nonet,M. and Wei,A. (1997) The impact of the *C.elegans* genome-sequencing project on K^+ channel biology. *Pflügers Arch.*, **434**, R79–R81.

Shen,K.Z., North,R.A. and Surprenant,A. (1992) Potassium channels opened by noradrenaline and other transmitters in excised membrane patches of guinea-pig submucosal neurones. *J. Physiol. (Lond.)*, **445**, 581–599.

Siegelbaum,S.A., Camardo,J.S. and Kandel,E. (1982) Serotonin and cyclic AMP close single K^+ channels in *Aplysia* sensory neurones. *Nature*, **229**, 413–417.

Siesjö,B.K. and Wieloch,T. (1985) Brain injury: neurochemical aspects. In Becker,D.P. and Povlishok,J.P. (eds), *Central Nervous System Trauma*. William Byrd Press Inc., Richmond, VA, pp. 513–532.

Siesjö,B.K., Agardh,C.D., Bengtsson,F. and Smith,M.L. (1989) Arachidonic acid metabolism in seizures. *Ann. NY Acad. Sci.*, **559**, 323–339.

Stutzmann,J.M., Böhme,G.A., Gandolfo,G., Gottesmann,C., Lafforgue,J., Blanchard,J.C., Laduron,P.M. and Lazdunski,M. (1991) Riluzole prevents hyperexcitability produced by the mast cell degranulating peptide and dendrotoxin I in the rat. *Eur. J. Pharmacol.*, **193**, 223–229.

Theander,S., Fahraeus,C. and Grampp,W. (1996) Analysis of leak current properties in the lobster stretch receptor neurone. *Acta Physiol. Scand.*, **157**, 493–509.

Villarroel,A. (1993) Suppression of neuronal potassium A-current by arachidonic acid. *FEBS Lett.*, **335**, 184–188.

Villarroel,A. and Schwarz,T.L. (1996) Inhibition of the Kv4 (Shal) family of transient K^+ currents by arachidonic acid. *J. Neurosci.*, **16**, 1016–1025.

Wagner,P.G. and Dekin,M.S. (1997) cAMP modulates an S-type K^+ channel coupled to GABA(B) receptors in mammalian respiratory neurons. *Neuroreport*, **8**, 1667–1670.

Wu,J.V., Rubinstein,T. and Shrager,P. (1993) Single channel characterization of multiple types of potassium channels in demyelinated *Xenopus* axons. *J. Neurosci.*, **13**, 5153–5163.

Yang,J., Jan,Y.N. and Jan,L.Y. (1995) Determination of the subunit stoichiometry of an inwardly rectifying potassium channel. *Neuron*, **15**, 1441–1447.

Yool,A.J. and Schwarz,T.L. (1991) Alteration of ionic selectivity of a K^+ channel by mutation of the H5 region. *Nature*, **349**, 700–704.

Yue,T.Y. and Marban,E. (1988) A novel cardiac potassium channel that is active and conductive at depolarized potentials. *Pflügers Arch.*, **413**, 127–133.

Received March 9, 1998; revised and accepted April 7, 1998